Proceedings of the National Conference on Computational Modeling of Fluid Dynamics Problems (CMFDP-2019)
NIT Warangal, India – Jan 18-20, 2019
Paper No. XXX (The number assigned when the papaer is accepted)

Computational analysis of Heat Transfer Performance of Jet Impingement Cooling on a flat surface

Mohamed Illyas[a*], B.R.Ramesh Bapu[b,] , V. Venkata Subba Rao[c]
[a]*Department of Mechanical Engineering, B S Abdur Rahman Crescent Institute of Science and Technology, Chennai -600073, India*
[b]*Department of Mechanical Engineering, Chennai Institute of Technology, Chennai 600069, India*
[c]*Department of Mechanical Engineering, Jawaharlal Nehru Technological University, Kakinada 533003, India*

*Corresponding author Email: illyas1978@gmail.com

Impinging jets are extensively employed for industrial cooling because of its higher surface heat transfer rate. The present study focuses on heat transfer and flow structure of swirling impinging jet with constant heat flux simulant chip. The simulant chip is impinged by swirling jet produced by a helical insert in the circular nozzle. The heat transfer performance and flow field are examined using computational fluid dynamics tool with Reynolds number range of 8000 - 23000 and dimensionless nozzle exit to impinging surface distance of H/D = 5 with varying thread interval of helical inserts. The heat transfer rate is evaluated by obtaining the Nusselt number distribution on the impinging surface. The result of the analysis reveals that helical insert with lower pitch distance exhibits radial uniformity in Nusselt number and also increased uniformity in radial velocity component with respect to jet axis. The increase in Reynolds number decreases the radial uniformity of Nusselt number at fixed H/D distance.

***Keywords*:** CFD**,** Heat Transfer, Jet Impingement, Swirling Jet

1. Introduction

Impinging jets are being employed in various engineering applications such as cooling of electronic components, turbine blades, drying of papers and garments. Jet impingement heat transfer is an effective way to provide localized heating or cooling. The jet impingement combined with recent technique of phase change cooling can also be used in near future because of its inherent low cost and robust. Higher heat and mass transfer rate with radial uniformity are required for applications like cooling of electronic components and chemical vapour deposition. This could be probably achieved by swirling impinging jet cooling. Swirling jets are characterized by tangential velocity components that produce a spiral shaped motion resulting in broadening of the impingement region as well as wall jet region; this feature is coupled, particularly near the stagnation region, with weakening of axial flux as well.

A swirling impinging jet has been designed for the first time by Ward and Mahmood [1] measured radial distribution of Nusselt number was relatively more uniform and its values were significantly lower. A swirling nozzle made on a cylinder with four narrow channels was developed by Huang and El Genk [2] and the experimental measurements reported the increase in the radial uniformity as well as surface average Nusselt number. Wen and Jang [3] designed swirling strips as insert for jet nozzle and showed that the crossed swirling strips has good heat transfer performance with respect to conventional circular jets. In the literature of swirling jets heat transfer data are reported only in terms of radial distribution even if the flow field behavior require two dimensional measurements. Lee and Won [4] analyzed the distribution of heat transfer with respect to swirling impinging jets and reported that the heat transfer uniformity depends on the swirl and it is assessed by a dimensionless number called swirl number. Yen et al. [5] employed liquid crystal technique to analyze the heat transfer over a ribbed surface for circular and elliptical array of jet. Mao Yu Wen [6] performed flow visualization study to examine the heat transfer characteristics of

a circular and swirling impinging jets and reported better heat transfer performance for swirling jet. Bakirci and Bilen [9] designed helical inserts which are placed in a circular hollow tube. The fluid passing in to tube is divided into multiple streams and rotated in a centre column based on the intensity of swirl. Certainly these designs have some limitations as the flow acts as a array of multiple jet and as they impinged on the target surface with some inclination, the heat transfer at the stagnation point is a relatively lower than a circular impinging jet. Hwang and Cheng [10] employed thermo chromic liquid crystal sheets to determine the convective heat transfer coefficients on side walls of a triangular duct with a swirling jet. Three different angles between the swirling jet and the duct axial direction were examined.

Most of the studies employed smooth surfaces for the impinging jet. Surface like printed circuit board frequently have obstacles on it. These obstacles greatly influence in changing the heat transfer and flow patterns. The objective of the current study is to investigate the influence of swirling impinging jet on flow and heat transfer over the rough surface. In the present study, the heat transfer from a flat surface to an impinging jet is investigated as a function of jet exit to surface distance (H/D = 5) and Reynolds number (8000-2300). The jet leaving a nozzle with helical inserts of varying pitch distances of 10 mm, 20 mm and 40mm are considered. The influence of flow structure on the convective heat transfer is also studied. The physical properties of Epoxy plate with copper foil (common material for printed circuit board) have been considered for impinging surface.

2. Computational Modeling

The computational domain of impinging jet system is shown in Fig.1. The diameter of the jet nozzle is D. The ratio of the impinging surface distance to the diameter of the jet H/D, is equal to 5. Selection of these variables is with respect to the study that under these conditions the confined boundary may strongly influence the jet flow.

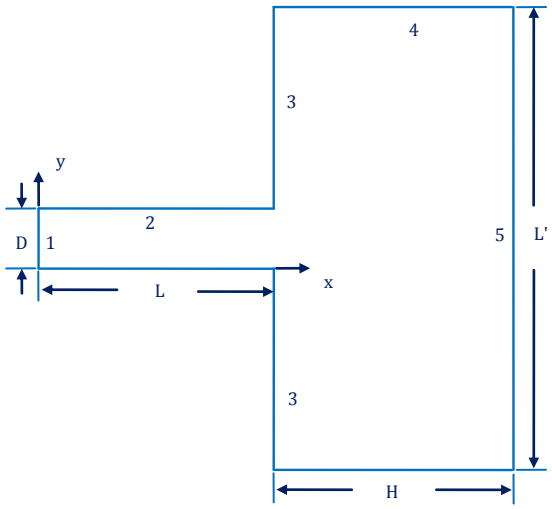

Fig. 1. Computational domain of impinging jet

The dimensions for the extended domain in Fig.1 are: L/D = 6.66 L'/D = 26.66. The following boundary conditions are specified : Boundary named 1 is the inlet of jet (x = 0 and y = D). The flow of jet is at a constant velocity and uniform temperature ($T = T_0$). Boundary 5 is the target wall (x= L+H) and constant heat flux ($q = q_x$) is imposed. The wall is assigned at constant temperature ($T = T_w$). Confined adiabatic wall with no slip conditions are specified for boundaries 2 and 3.
At the exit of the channel (Boundary 4, y = D/2+L'/2) a constant pressure P is applied as shown in fig.1 Boundary 5 (Impinging surface) is assigned with rough wall boundary condition with roughness height 0.5 mm and no slip condition is assigned for "Wall Influence On Flow".

3. Grid Independency

The domain was discretized with an unstructured tetrahedral mesh with refined mesh at the impinging surface and at nozzle exit for considering the effect of exit flow structure.

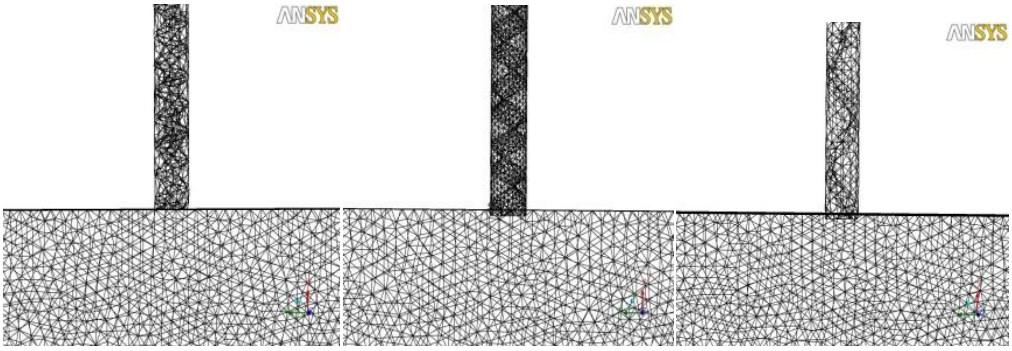

Fig. 2. Discretized domain of impinging jet

Optimization of meshing element is essential to attain a balance between the computing time and the solution accuracy. Initially the domain is discretized with 3.57, 4.82, 6.52, 8.06 and 9.68 million elements. It is observed that velocity contours of 3.57, 4.82 and 6.52 million are different those of 8.06 and 9.68 million elements. The latter two are good agreement with each other. Considering the lesser computing time the domain with 8.06 million elements is selected over the one with 9.68 million elements.

4. Turbulence Model

The standard k-ϵ turbulence model is the most widely used and validated one among the k-ϵ models. It has attained a remarkable successes in computing a wide variety of thin shear layer flows. However, its performance is not effective in the strained flows (swirling or rotating flows and curved boundary layers). Alternatively, the RNG k-ϵ turbulence model is comparable with standard k-ϵ model except for some added refinements to enhance the accuracy for such rotating or swirl flows. Besides, studies reported that the Realizable k-ϵ model performs better in solving fluid dynamic problems. Nevertheless, the Realizable k-ϵ model yet to establish its performance in line with the RNG k-ϵ model. The RNG k-ϵ model is relatively more receptive to strain flows than other two k-ϵ models. Moreover, it accounts the effect of swirl in turbulence flow, thereby increasing the accuracy for swirling flows. As a result, the RNG k-ϵ model is preferred for strained flows with a confined jet in the domain,. The transport equations of RNG k-ϵ is given as follows

$$\frac{\partial}{\partial t}(\rho k) + \frac{\partial}{\partial x_i}(\rho k u_i) = \frac{\partial}{\partial x_j}\left[\nu_k \mu \frac{\partial k}{\partial x_j}\right] + M_k + M_b - \rho\epsilon - Y_m + Y_k \quad (1)$$

$$\frac{\partial}{\partial x_i}(\rho \varepsilon u_i) = \frac{\partial}{\partial x_j}\left[\nu_\epsilon \mu \frac{\partial \varepsilon}{\partial x_j}\right] + C_{le}\frac{\varepsilon}{k}(M_k + C_{3\varepsilon}M_b) - C_{2e}\rho\frac{\varepsilon^2}{k} - N_\epsilon + Y_\varepsilon \quad (2)$$

while ρ denotes density of fluid, k and ϵ represent the kinetic energy and dissipation rate respectively, u is the velocity, μ is the effective viscosity, ν_k and ν_ε are the inverse effective Prandtl number for the k and ϵ terms, M_k is the generation of turbulent kinetic energy as a result of velocity gradient, M_b is the turbulent kinetic energy as result of buoyancy effect, Y_k is source term for k *and* and Y_ε source term for ϵ. N_ε is an additional term in the RNG κ-ε model which is modeled by

$$N_\varepsilon = \frac{C_\mu \rho \eta^3 (1-\frac{\eta}{\eta_0})\varepsilon^2}{1+\beta\eta^3}\frac{\varepsilon^2}{k} \quad (3)$$

By substituting (3) in Eq. (2), the Eq. (2) can be written as

$$\frac{\partial}{\partial t}(\rho \varepsilon) + \frac{\partial}{\partial x_i}(\rho \varepsilon u_i) = \frac{\partial}{\partial x_j}\left[\nu_\epsilon \mu \frac{\partial \varepsilon}{\partial x_j}\right] + C_{le}\frac{\varepsilon}{k}(M_k + C_{3\varepsilon}M_b) - C_{2e}\rho\frac{\varepsilon^2}{k} + \frac{C_\mu \rho \eta^3 (1-\frac{\eta}{\eta_0})\varepsilon^2}{1+\beta\eta^3}\frac{\varepsilon^2}{k} + Y_\varepsilon \quad (4)$$

Where $\eta = \frac{S_k}{\varepsilon}$, $\eta_0 = 4.38$ and $\beta = 0.012$
Where C_{le} = 1.42 and C_{2e} = 1.68

5. Results and Discussion

5.1 Effect of Swirl and Non swirl

The Nusselt number distribution over the impinging surface for swirling and non swirling jet for Re = 8000, 1500 and 23000 at H/D = 5 is shown in fig. 3. The non swirling jet exhibits higher Nusselt number in the impingement region compared with swirling jet as shown in fig. 3. This is fact is due to the prevailing potential core at jet exit (Viskanta [20]) maintains uniform velocity whereas enhanced turbulence with the interaction of swirling flow reduces the arrival velocity of jet nearing the impinging surface. The decrease in Nusselt number with increasing radial distance on the impinging surface is observed for non swirling jet. This is due to development of boundary layer caused by the raising velocity gradient (Zukerman and Lior [21]). The uniform distribution of Nusselt number prevails over the target surface for swirling jet with decrease in its magnitude compared with non swirling jet.

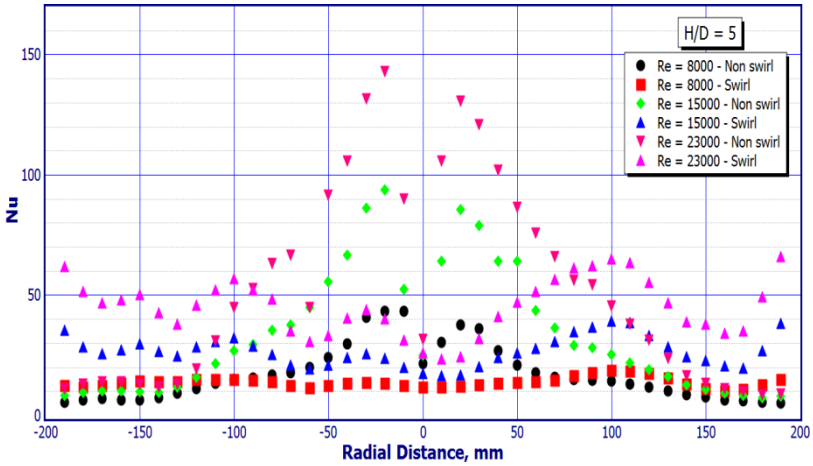

Fig. 3. Nusselt number variation for swirling and Non swirling jet at H/D = 5

The higher heat transfer uniformity is attributed to the enhanced spreading rate of swirling jet as reported by Dae Hee Lee et al. [22]. The magnitude of Nusselt number increases with increasing Reynolds number for both swirling and non swirling flows due to higher arrival velocity of the jet near the impinging surface. However the effect of swirl with increased velocity of the swirling jet entrain more atmospheric air on the target surface which may further enhance the heat transfer rate as described by Huang and El Genk [2].

5.2 Effect of pitch distance

The distribution of Nusselt number for the swirling jet with varying pitch distance is shown in fig.4 The swirling jet with lower pitch distance (P = 10 mm) exhibits relatively higher spreading rate resulting in more uniform distribution of Nusselt number with lower magnitude as shown in fig.4 compared with jet leaving the inserts with 20 mm and 40 mm pitch. The reduction in Nusselt number is due to the higher spreading rate of the jet causes losing of its original momentum. Besides, the insert with lower pitch enhances the swirling effect of jet spreading outward radially through the atmospheric air when it nearing the impinging surface.

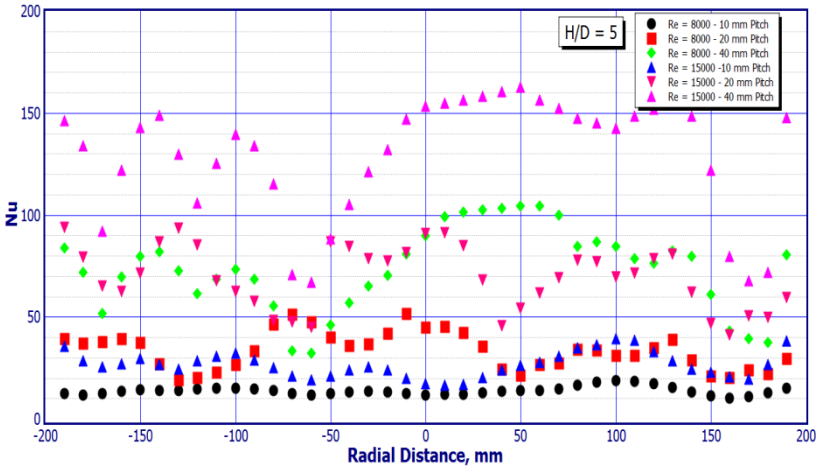

Fig. 4. Nusselt number variation for swirling jet at varying pitch distances for H/D = 5

The swirling jet leaving insert with 40 mm pitch exhibits higher value of stagnation point heat transfer and reduced heat transfer rate in the wall jet region for Re = 15000 as shown in fig. 4. The higher stagnation point heat transfer is due to higher axial momentum of the jet compared with jet with 10 mm and 20 mm pitch. The increase in Reynolds number for the swirling jet increases the heat transfer rate with the reduction in heat transfer uniformity as shown in fig.4. The increase in heat transfer is attributed to the higher jet arrival velocity on the impinging surface as reported earlier.

5.3 Exit Flow structure

The exit flow structures of annular swirling impinging jet have been discussed in this section. The exit flow pattern of swirling and non swirling jet interms of velocity vector at H/D = 5 is shown in fig. 5. The exit flow acquires radial velocity components due to the presence of swirl and it diverges radially on leaving the annular nozzle. The flow field of swirling jet shows the increased uniformity in the radial velocity component with respect to nozzle axis. Strong recirculation zones have been observed in swirling jet. The presence of recirculation zone is due to swirling effect which produces axial pressure gradient near the jet exit as reported by Andrea Ianiro [23]. This phenomenon causes lower heat transfer at the centre of impinging surface resulting in reduced stagnation Nusselt number.

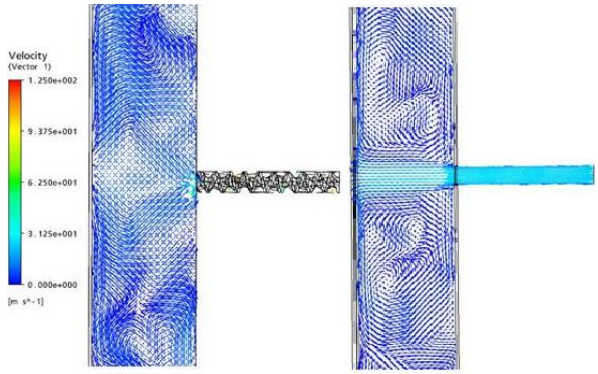

Fig. 5. Velocity vector for swirl and non swirl flows at H/D = 5

The presence of two shear layers are observed for the swirling jet, one in the outer region between the jet and atmospheric air and other in the region between the jet and recirculation zone as shown in fig.5 a. which is an agreement with results of Fenot et al. [24]. The presence of potential core is apparent for the non swirling jet as the flow is not stirred up in the free jet as shown in fig.5 b The

existence of radial velocity component of non swirling jet is minimal causing relatively lower turbulence in the flow field. The reverse flow in both the cases causes recirculation zones in the flow as shown in fig.5 a and b. The exit flow patterns of swirling jet with varying pitch distances at H/D = 5 are shown in fig. 6. The presence of stronger recirculation zones at lower pitch distances substantiates more intense shear layer as observed in fig. 6 a. The distribution flow field shows that the cross flow effect is significant at lower pitch distances. The increased uniformity of the radial velocity component is observed for the jet leaving the insert with 10 mm pitch with respect to nozzle axis.

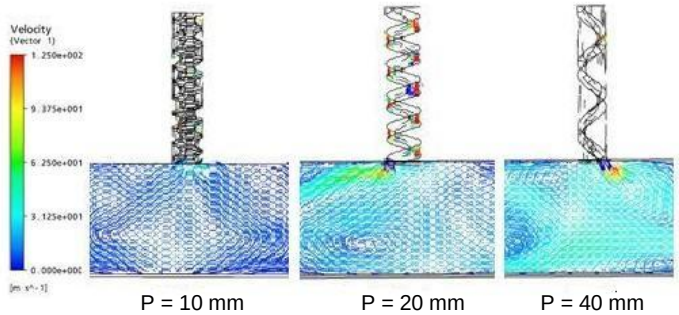

Fig. 6. Velocity vector for varying pitch distance

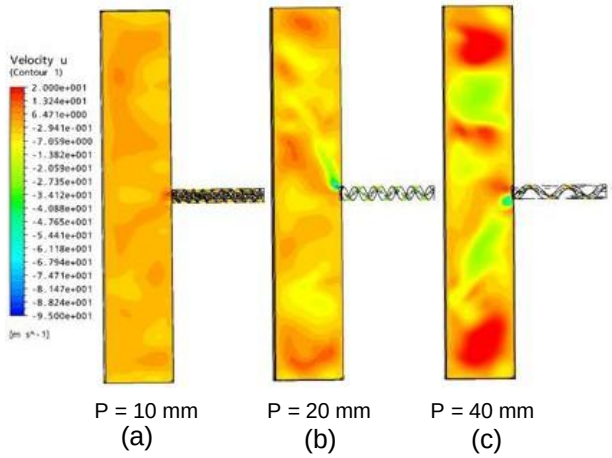

Fig. 7. Distribution of axial velocity component

Figure 7 shows the distribution of axial velocity components for the swirling jet with varying pitch distances. The concentrated axial velocity components is observed for the jet with 40 mm pitch (fig. 7 c) when the reverse flow occurs. The intensity has reduced at 20 mm pitch distance as shown in fig. 7 b. The concentration has reduced further in the case of 10 mm pitch (fig. 7 a) resulting in uniform distribution over the entire flow field.

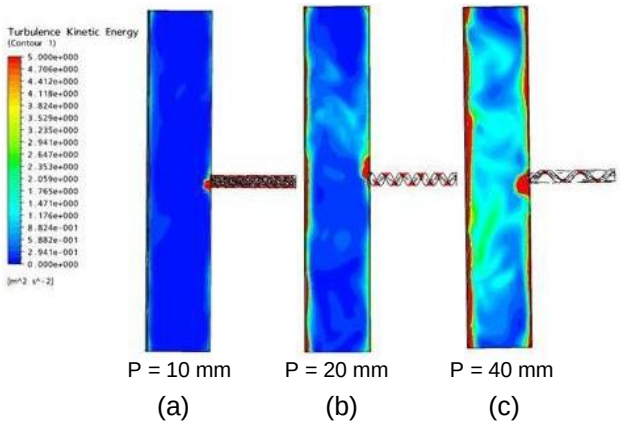

Fig. 8. Turbulence Kinetic Energy variation

This fact indicates the uniform spreading of jet which may imply positive impact on the heat transfer over the impinging surface. The turbulence kinetic energy variation for the swirling jet is shown in fig. 8. The turbulence kinetic energy characterizes measured root mean square velocity fluctuations and it represents the intensity of turbulence. The momentous increase in turbulent kinetic energy implies higher mixing rate for the swirling jet. This is due to the intense momentum exerted by the swirling jet. The intensity of turbulence is higher at 40 mm pitch (fig. 8 a) particularly in the vicinity of recirculation regions which may increase the heat transfer rate. Concentration of turbulence intensity has decreased in the 20 mm pitch and 10 mm pitch inserts as shown in fig.8 b a. This may significantly increase the uniformity in heat transfer.

6. Conclusion

Thus the heat transfer and flow characteristics of swirling impinging jet are studied and following conclusions is drawn

- Increased uniformity in the distribution of Nusselt number has been observed in the swirl flow compared with non swirl flow with relatively lower values of Nusselt number.
- The increase in pitch distance increases the value of Nusselt number with the reduction in radial uniformity of heat transfer.
- The uniformity of Nusselt number distribution decreases with increase in Reynolds number.
- The radial velocity component and intensity of turbulence remain uniform at lower pitch distance.

References

[1] J. Ward, M. Mahmood, Heat transfer from a Turbulent, swirling impinging jet, Proceedings of the 7th International Heat Transfer Conference. 3, 401- 407 (1982) Munich, West Germany.

[2] L. Huang and M. S. El-Genk, Heat transfer and flow visualization experiments of swirling, multi-channel, and conventional impinging jets. International Journal of Heat and Mass Transfer. 41, 583-600 (1998)

[3] M. Y. Wen and K. J. Jang, An impingement cooling on a flat surface by using circular jet with longitudinal swirling strips. International Journal of Heat and Mass Transfer. 46, 4657- 4667 (2003)

[4] D. H. Lee, S. J. Won, Y. T. Kim and Y. S. Chung, Turbulent Heat Transfer from a flat surface to a swirling round impinging jet. International Journal of Heat and Mass Transfer. 45, 223-227 (2002)

[5] W.M. Yan, S.C. Mei, H.C. Liu, C.Y. Soong, W.J. Yang, Measurement of detailed heat transfer on a surface under arrays of impinging elliptic jets by a transient liquid crystal technique. International Journal of Heat and Mass Transfer. 47, 5235– 5245 (2004)

[6] Mao-Yu Wen, Kuen-Jang Jang, An Impingement Cooling on A Flat Surface by Using Circular Jet with Longitudinal Swirling Strips. International Journal of Heat and Mass Transfer. 46, 4657-4667 (2003)

[7] W.M. Yan, S.C. Mei, Measurement of detailed heat transfer along rib-roughened surface under arrays of impinging elliptic jets, International Journal of Heat and Mass Transfer. 49, 159–170 (2006)

[8] M.E. Arzutug, S. Yapici, M.M. Kocakerim, A Comparison of mass transfer between a plate and submerged conventional and multichannel impinging jets. International Communication in Heat Mass Transfer. 32, 842–854 (2005)

[9] K. Bakirci, K. and K. Bilen, Visualization of heat transfer for impinging swirl flow. Experimental Thermal and Fluid Science. 32, 182-191 (2007)

[10] J.J. Hwang, C.S. Cheng, Augmented heat transfer in a triangular duct by using multiple swirling jets. ASME Journal of Heat Transfer. 121, 683–690 (1999)

[11] John C. Duda, Francis D. Lagor, A flow visualization study of the development of vortex structures in a round jet impinging on a flat plate and a cylindrical pedestal. Experimental Thermal and Fluid Science. 32 (8): 1754–1758 (2008)

[12] Chen Yu-Yang, Yuan Zhong- Xian, Ma Chong-Fang, Experimental Study of Heat Transfer of Swirling Jet Impingement with Liquid Crystal Technique. Journal of Engineering Thermo physics. 24, 646-648 (2003)

[13] A. K. Gupta, D.G. Lilley and N. Syred, Swirl Flows. Abacus press, Cambridge Massachusetts (1984)

[14] Hwa Chong Tien and Wei-Dong Huang, Simulation and assessment of air impingement cooling on squared pin-fin heat sinks applied in personal computers. Journal of Marine Science and Technology. 13, 20-27 (2005)

[15] K. Oliphant, B.W. Webb, An experimental comparison of liquid jet array and spray impingement cooling in the non-boiling regime. Experimental Thermal and Fluid Science. 18,1-10 (1998)

[16] Gregory J. Michna Eric A. Browne Yoav Peles. 2009. Single-Phase Microscale Jet Stagnation Point Heat, Transfer. ASME Journal of Heat Transfer. 131, 111402- 1-8 (2009)

[17] D.W. Zhou, Sang-Joon Lee, Heat transfer enhancement of impinging jets using mesh screens. nternational Journal of Heat and Mass Transfer. 47, 2097-2108 (2004)

[18] David J. Sailor, Daniel J. Rohli, Effect of variable duty cycle Flow pulsations on heat transfer enhancement for an impinging air jet. International Journal of Heat and Fluid Flow. 20, 574 - 580 (1999)

[19] Z.X.Yuan, Y.Y.Chen, J.G. Jiang, Swirling effect of jet impingement on heat transfer from a flat surface to CO_2 stream. Experimental Thermal and Fluid Science 31,55-60 (2006)

[20] R. Viskanta, Heat Transfer to Impinging Isothermal Gas and Flame Jets. Experimental Thermal and Fluid Science 6, 111-134 (1993)

[21] N. Zuckerman and N. Lior. Jet impingement heat transfer: physics, correlations, and numerical modeling, Advances in Heat Transfer 39, 565-631 (2006)

[22] Dae Hee Lee, Se Youl Won, Yun Taek Kim and Young Suk Chung, Turbulent heat transfer from a flat surface to a swirling round impinging jet. International Journal of Heat and Mass Transfer 45, 223-227 (2002)

[23] Andrea Ianiro and Gennaro Cardone Heat transfer rate and uniformity in multichannel swirling impinging jets. Applied Thermal Engineering 49, 89-98 (2012)

[24] M. Fenot, E. Dorignac and G. Lalizel, Heat transfer and flow structure of a multichannel impinging jet. International Journal of Thermal Sciences 90, 323-338 (2015)